FIBER - REINFORCED HIGH – PERFORMANCE CONCRETES EXPOSED TO HIGH TEMPERATURE: MATERIALS BEHAVIOR AND STRUCTURAL IMPLICATIONS

Francesco Lo Monte (1), Pietro G. Gambarova (1), Zhijin Xu (2) and Yuhang Li (3)

(1) Dept. of Civil and Environmental Engineering, Politecnico di Milano, Milan, Italy

(2) School of Civil Engineering, Jiaotong University, Beijing, China

(3) College of Civil Engineering, Tongji University, Shanghai, China

Abstract

The many studies devoted in the last twenty years to high strength/high performance concrete (HSC/HPC) demonstrate its very interesting properties in terms of stiffness, strength and durability. These *pluses*, however, are partly counterbalanced by a few *minuses* (such as greater brittleness at room temperature and greater heat sensitivity), that can be reduced – and even zeroed – by introducing fibers, which improve concrete toughness at any temperature (steel fibers) and durability at high temperature (mainly polymeric fibers).

Since many are the parameters affecting concrete properties at high temperature, keeping constant the volumetric fraction of the cementitious matrix (as done in this research project) is a must whenever different fibrous mixes are to be compared. To have further information on the role of steel and polymeric fibers on HSC/HPC behavior at high temperature, seven mixes have been investigated in terms of thermal diffusivity, stress-strain curves in compression and elastic modulus (f_c = 60 MPa; T = 20-750°C, *hot* and *residual* conditions). Among polypropylene fibers, fibrillated fibers have an edge over monofilament fibers in residual conditions, while steel fibers are the most effective in both hot and residual conditions.

A structural application is presented as well, concerning two R/C columns (with/without steel fibers) subjected to standard fire, where the structural behavior at any fire duration is enhanced thanks to the extra ductility provided by the fibers.

1. INTRODUCTION

High-Performance Concrete in its many forms is still a rather *young* material (a little more than twentyfive-year old!), whose very interesting properties in terms of stiffness, strength and durability are counterbalanced – at least partly – by a greater brittleness at room temperature and a greater sensitivity at high temperature ([1-3], see Shah and Ahmad in "High-Performance Concrete: Properties and Applications", McGraw-Hill, 1994, and Nawy in "Fundamentals of High-Performance Concrete", John Wiley & Sons, 2000). The minuses,

however, can be reduced – even markedly – by introducing rather low amounts of fibers, which improve concrete toughness (steel fibers) and high-temperature performance (steel and polymeric fibers ([4, 5] see Bentur and Mindess in "Fiber-Reinforced Cementitious Composites", Modern Concrete Series, 2006). In spite of the many books and papers written on plain and fibrous HSC/HPC, the correlation between the macro level (physical and mechanical properties, cracking) and the micro/meso level (constituents, interfaces, cement chemistry, micro-cracking) is still a challenge, which requires concrete macro properties to be well known to properly address the research activity at the meso/micro level. Within this context, further information on the high-temperature behavior of high-performance fiber-reinforced concrete is provided here by investigating seven concrete mixes within a research project still in progress in Milan (f_c = 60 MPa, plain concrete and concretes containing pp fibers of different type, and steel fibers with different contents [6]).

In the second part, using steel fibers in the mix is shown to enhance the structural performance of R/C columns in fire (a *hot* topic indeed [7]!). A numerical example is worked out following a previous study [8], to compare two columns (with/without fibers), by implementing the constitutive laws of steel fiber-reinforced concrete at high temperature.

2. CONCRETE MIXES

In a rather comprehensive research project still in progress in Milan [6], eleven mixes have been investigated both at high temperature and in residual conditions, including 3 grades (f_c = 40, 60, 90 MPa; f_{cc} = 48, 70, 100 MPa), 3 aggregate types (mixed = silico-calcareous, calcareous and basalt aggregates) and 3 fiber types (pp fibers – monofilament and fibrillated – and steel fibers). Seven of the mixes, however, concern the intermediate-grade concrete (f_c = 60 MPa), that is the subject of this paper. Beside room temperature (20°C), 4 temperatures were considered for testing in both *hot* and *residual* conditions (105, 250, 500 and 750°C). Among the *hot* tests, however, only those at 500 and 750°C have been carried out so far and are presented in the following. (Note that not all mixes were subjected to all tests).

In Table 1 the mix design and the compressive strength of the seven mixes considered in this paper are reported. Note that in all mixes the volumetric fraction of the cementitious matrix is the same, as heat sensitivity depends mainly on the chemo-physical processes occurring in the cementitious matrix.

Table 1: Mix designs of the seven concretes considered in this paper

Mix designation →	70S	70S-PM05	70S-PM1	70S-PM2	70S-PF2	70S-SF40	70S-SF60
CEM I 42.5R + GGBS* (kg/m^3)	400 + 200						
Mixed aggr. d_a = 16 mm (kg/m^3)	1559						
ppm$^{\wedge}$, ppf$^{\wedge\wedge}$,stf$^{\wedge\wedge\wedge}$ fibers (kg/m^3)	-	0.5$^{\wedge}$	1.0$^{\wedge}$	2.0$^{\wedge}$	2.0$^{\wedge\wedge}$	40$^{\wedge\wedge\wedge}$	60$^{\wedge\wedge\wedge}$
Acrylic superplast. (kg/m^3)	2.76						
Water/binder ratio w/b (-)	0.36						
Density at the fresh state (kg/m^3)	2390	2380	2370	2350	2390	2410	2430
f_c/f_{cc} at 28 days (MPa)	62/72	63/70	60/70	60/69	61/72	63/72	60/73

($^{\wedge}$) pp monofilament fibers: extruded straight fibers treated with a surfactant, L = 12 mm, ∅ = 20 μm, L/∅ = 600.

($^{\wedge\wedge}$) pp fibrillated fibers: straight fibers cut from stripes with rectangular section , L = 12 mm, $\varnothing_{eq}$ = 48 μm, L/$\varnothing_{eq}$ = 250.

($^{\wedge\wedge\wedge}$) hooked steel fibers, L = 35 mm, ∅ = 550 μm, L/∅ = 64. (*) Ground Granulated Blast-furnace Slag.

3. SPECIMENS, THERMAL CYCLES AND INSTRUMENTATION

3.1 Residual tests

For each mix, eleven cylinders were cast, i.e. two *short* cylinders to be tested in compression per each reference temperature (∅ = 100 mm, h = 200 mm, Fig. 1a) and one *long* cylinder (∅ = 100 mm, h = 300 mm), that was instrumented with two thermocouples to evaluate the thermal diffusivity up to 950°C, see Fig. 2a. (Both thermocouples were placed in the mid-height section, one along the axis and the other at 5 mm from the lateral surface). Both heating and cooling were very slow (+1 and -0.25°C/minute).

The tests in compression were displacement-controlled (strain rate = 0.2–1.0 • 10^{-4}/s; initial stress rate = 0.4-0.8 MPa/s). The shortening of the specimens was measured locally via 3 DD1 strain gauges placed at 120° astride the mid-height section (base length 50 mm); moreover, 3 LVDTs measured the plate-to-plate distance to monitor the post-peak behavior (Figs. 1a,b).

The elastic modulus was evaluated on the basis of the stress-strain curves in compression, as *secant modulus* ($\sigma_c \leq 0.4 f_c$). A 1000 kN-Schenck press was used in all residual tests.

3.2 Hot tests

For each mix ten short cylinders were cast to be tested in compression (two cylinders per each temperature and mix). According to the so-called *pre-heating technique* used in this project, each specimen is first wrapped up in an insulating *blanket* and then introduced into the furnace in batches of 4 specimens (Fig. 1d). After heating up to the reference temperature and resting at that temperature for two hours, the first specimen is extracted and tested in compression, followed by the other specimens at intervals comprised between 15 and 20 minutes, because each test requires less than ten minutes to attain the peak stress and five extra minutes to go through softening. (The heat loss is minimal in the first 8-10 minutes [9]).

Only the three LVDTs were used to evaluate the overall longitudinal strain, because gluing the DD1s to the lateral surface is pointless due to the high-temperature environment. Hence, to work out the local strain (at mid height) from the overall longitudinal strain, a correlation had to be established between the strain values provided by the two sets of instruments (LVDTs and DD1s). This correlation was based on the measurements obtained by repeating the tests at 20°C (virgin specimens), something that had to be done because of the different press used in the hot tests (press CONTROLS, capacity 2500 kN).

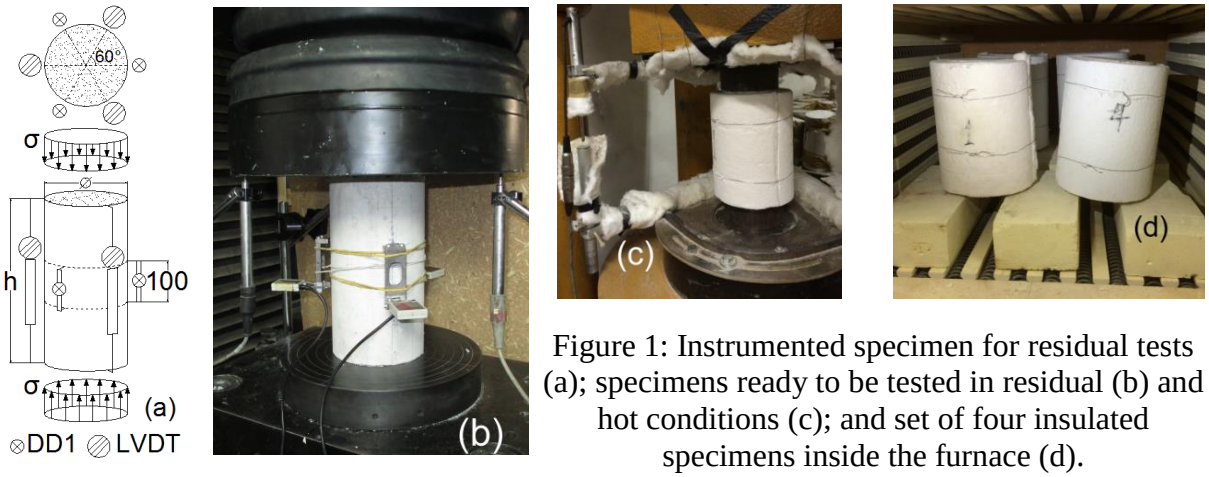

Figure 1: Instrumented specimen for residual tests (a); specimens ready to be tested in residual (b) and hot conditions (c); and set of four insulated specimens inside the furnace (d).

4. TEST RESULTS

4.1 Thermal diffusivity

As it is well known, the thermal parameter controlling heat transmission by conduction* is the thermal diffusivity D, that is the ratio between the heat transmitted and the heat stored by the unit mass of the material in question (* provided that the thermal conductivity is constant or quasi constant in time and space). D is defined as $\lambda/(c \cdot \rho)$, where λ is the thermal conductivity, c is the specific heat and ρ is the mass per unit volume. In a long cylinder ($h \geq 2\varnothing$) subjected to a constant heating rate v_h, the thermal diffusivity can be evaluated as:

$$D = v_h R^2/(4 \Delta T) \quad (1)$$

where $\Delta T = T_2 - T_1$ is the difference between the temperatures measured in two points (at 5 mm from the surface and along the axis at mid-height), while R is their distance (45 mm, Figs. 2a,b). In Fig. 2c, with reference to four of the seven mixes investigated in this study, the fibrous mixes are shown to have a slightly higher thermal diffusivity compared to the white mix (pp fibers facilitate free-water expulsion at rather low temperatures, and steel fibers tend to increase concrete thermal conductivity at any temperature).

4.2 Stress-strain curves and normalized diagrams

The stress-strain curves of four of the seven mixes investigated in this project are plotted in Fig. 3, for both residual and hot conditions. Beside the curves of the white mix (Mix 70S, Figs. 3a,b), only those of Mix 70S-PM2 are plotted (Figs. 3c,d) among the three mixes with pp monofilament fibers, as the behaviors of Mixes 70S-PM05 and 70S-PM1 differ only marginally from that of Mix 70S-PM2. Since the same applies to Mixes 70S-SF40 and 70S-SF60 containing steel fibers, only the curves of the former mix are plotted in Figs. 3g,h.

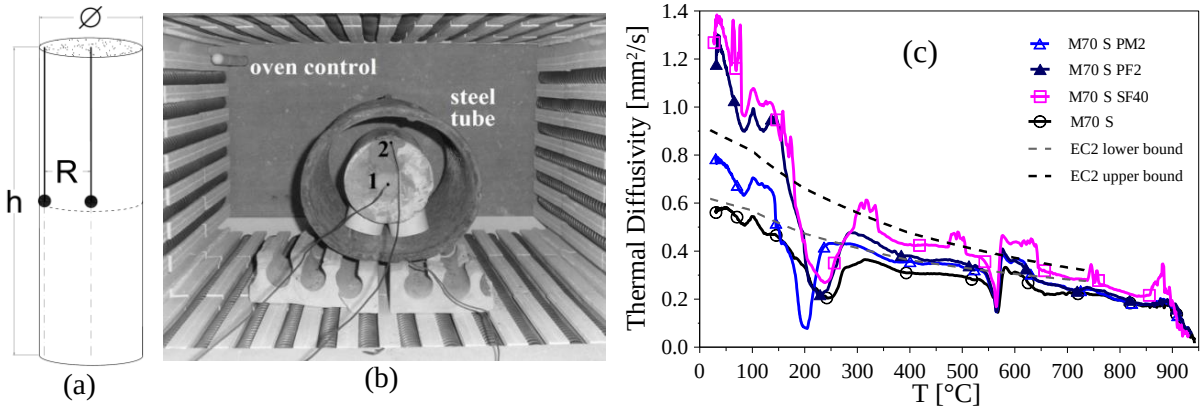

Figure 2: Thermal diffusivity: (a) thermocouples inside a specimen (●); and (b) diagrams.

Comparing the residual and hot behaviors (Figs. 3 and 4), what stands out clearly is the better behavior at high temperature, something that is well known and is confirmed here for all mixes. For instance, at 500°C the mean value (all mixes) of the normalized compressive strength is close to 1/3 in residual conditions and to more than 1/2 in hot conditions. In residual conditions, pp monofilament fibers appear to give no advantages compared to the white mix, while pp fibrillated fibers behave better and steel fibers much better, as their normalized strength is close to 35% and 41%, respectively (compared to 28% in the white mix).

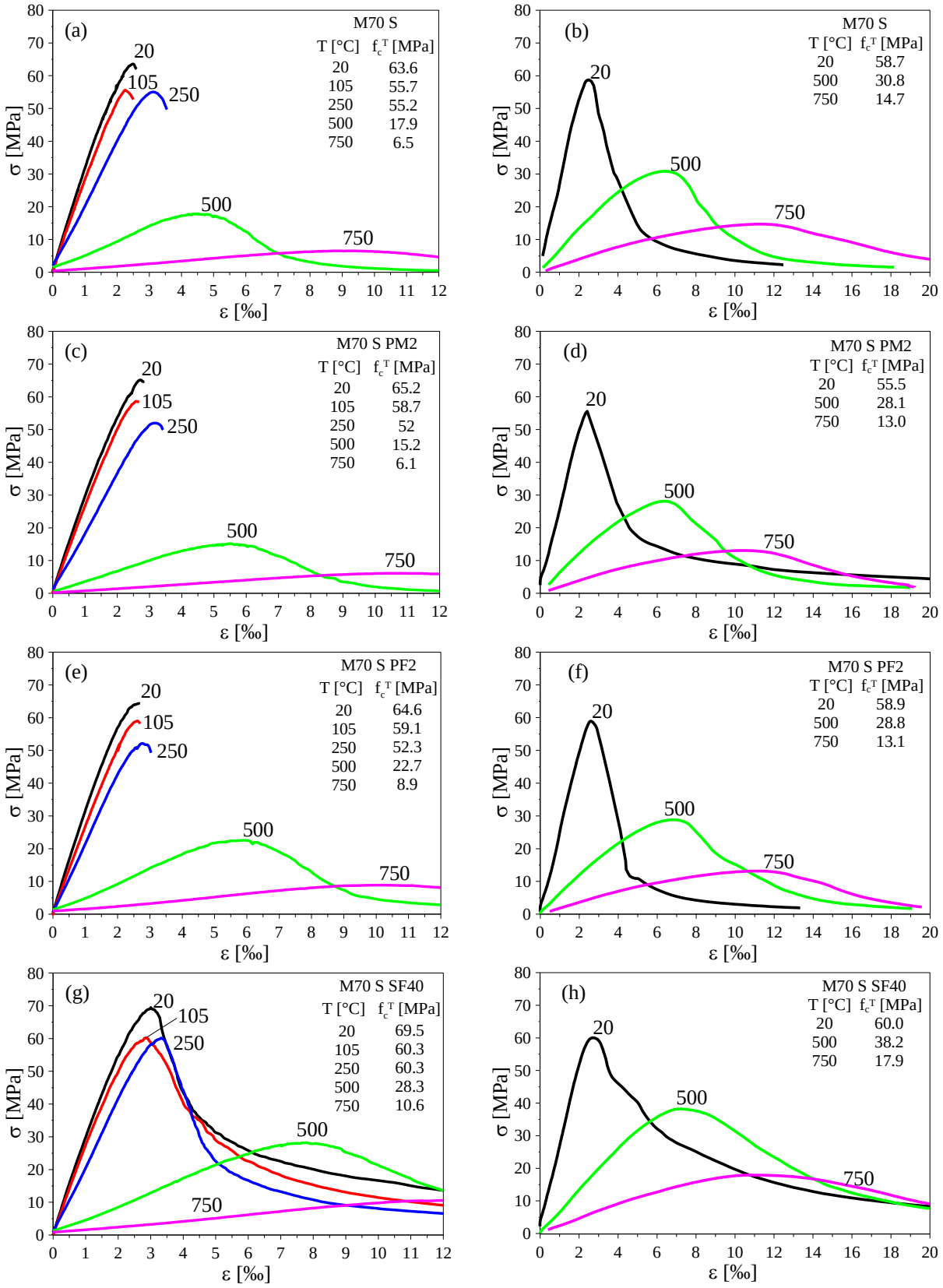

Figure 3: Stress-strain curves in residual (a,c,e,g),and in hot conditions (b,d,f,h) for 4 mixes.

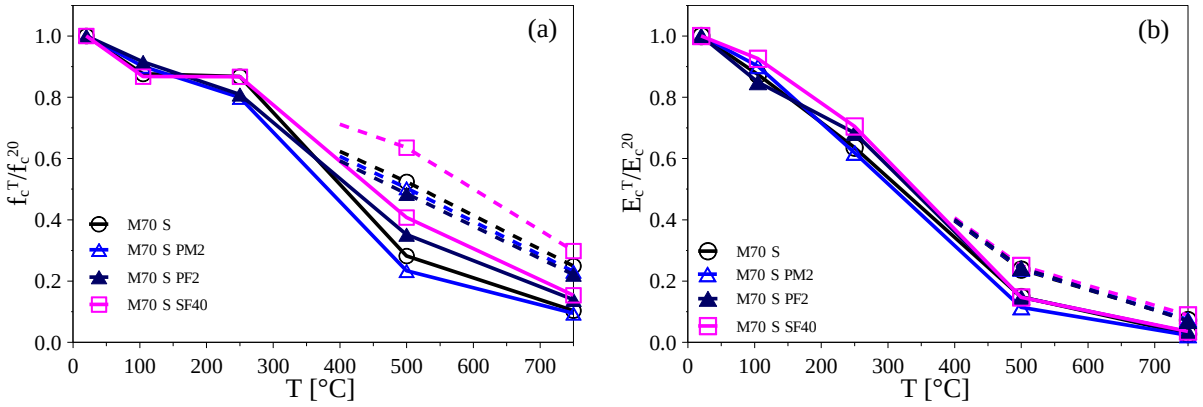

Figure 4: Normalized diagrams of the compressive strength (a), and of the secant elastic modulus (b); continuous/dashed curves refer to residual/hot tests.

In hot conditions, pp fiber-reinforced mixes behave similarly to the white mix (their strength is still close to 50% of the initial strength), while steel fibers are definitely more effective (66% of the initial strength) and increase substantially the ductility of the material.

In terms of strain at the peak stress, the values are comprised between 2‰ and 10-14‰ (20-750°C) without major differences among the different mixes. As for the elastic modulus, the largest decay occurs above 250°C, more in residual tests than in hot tests, due to the cooling-induced extra damage (Fig. 4b). Fibrous mixes have still an edge over the white mix.

5. STRUCTURAL APPLICATION

Two reinforced-concrete square columns subjected to an eccentric axial force (section 300x300 mm, 8∅12 mm bars, steel ratio 1%, height 3.0 m, eccentricity 1/300 of the height, pinned extremities, Fig. 5c) have been studied assuming the four faces to be exposed to the standard fire ISO 834. The concrete of the first column is plain (no fibers, Mix 70S), while the concrete of the second column is steel fiber-reinforced (v_f = 0.5%, 40 kg/m^3, Mix 70S-SF40).

The same approach and numerical procedure used in [8] has been adopted, by introducing the stress-strain relationships found in this project (see Figs. 3a,b and Figs. 3g,h); the experimental curves have been given analytical formulations based on EC2, considering the exponent of the term related to the instantaneous load-induced strain ε_σ as a function of the temperature (Figs. 5a,b for Mixes 70S and 70S-SF40, respectively). For the softening branch, a nonlinear curve (from EC2) and a logarithmic curve have been introduced for Mixes 70S and 70S-SF40, respectively. As indicated in the insert of Fig. 5a, the total strain ε_{tot} is the sum of three contributions: instantaneous load-induced strain ε_σ, transient strain ε_{tr} (which includes the creep strain) and thermal strain ε_{th}. The thermal strain is introduced according to EC2, while the transient strain is based on the well-known Anderberg and Thelandersson Model (1976), assuming k_{tr} = 2 and $\sigma = E_c\varepsilon_\sigma$.

The lateral displacement at mid-height is plotted in Fig. 5c, where the displacement of the fiber-reinforced column (thin curve) is shown to be slightly smaller than that of the plain-concrete column (thick curve). Both displacements diverge at the collapse of the columns, but the fibrous column has a fire resistance 10% higher (110' instead of 100').

The greater fire resistance of the fibrous column is confirmed by the intersections of the diagrams of the resisting moments (M_r) and of the applied moment (M_e) – Fig. 5d, the latter

being always an increasing function of fire duration because of 2nd-order displacements. The collapse is indicated by the divergence of the applied moment, that is associated with the divergence of the lateral displacement.

The M – N envelopes (Fig. 5e) show that the advantage offered by the fibers is rather limited (roughly +5% more resistance in pure compression and up to +20% under eccentric compression for a fire duration of 120'). The moment-curvature diagrams (Fig. 5f) confirm the sizable increase of the ductility of a heavily-loaded column, at any fire duration, this being definitely the plus offered by steel fibers.

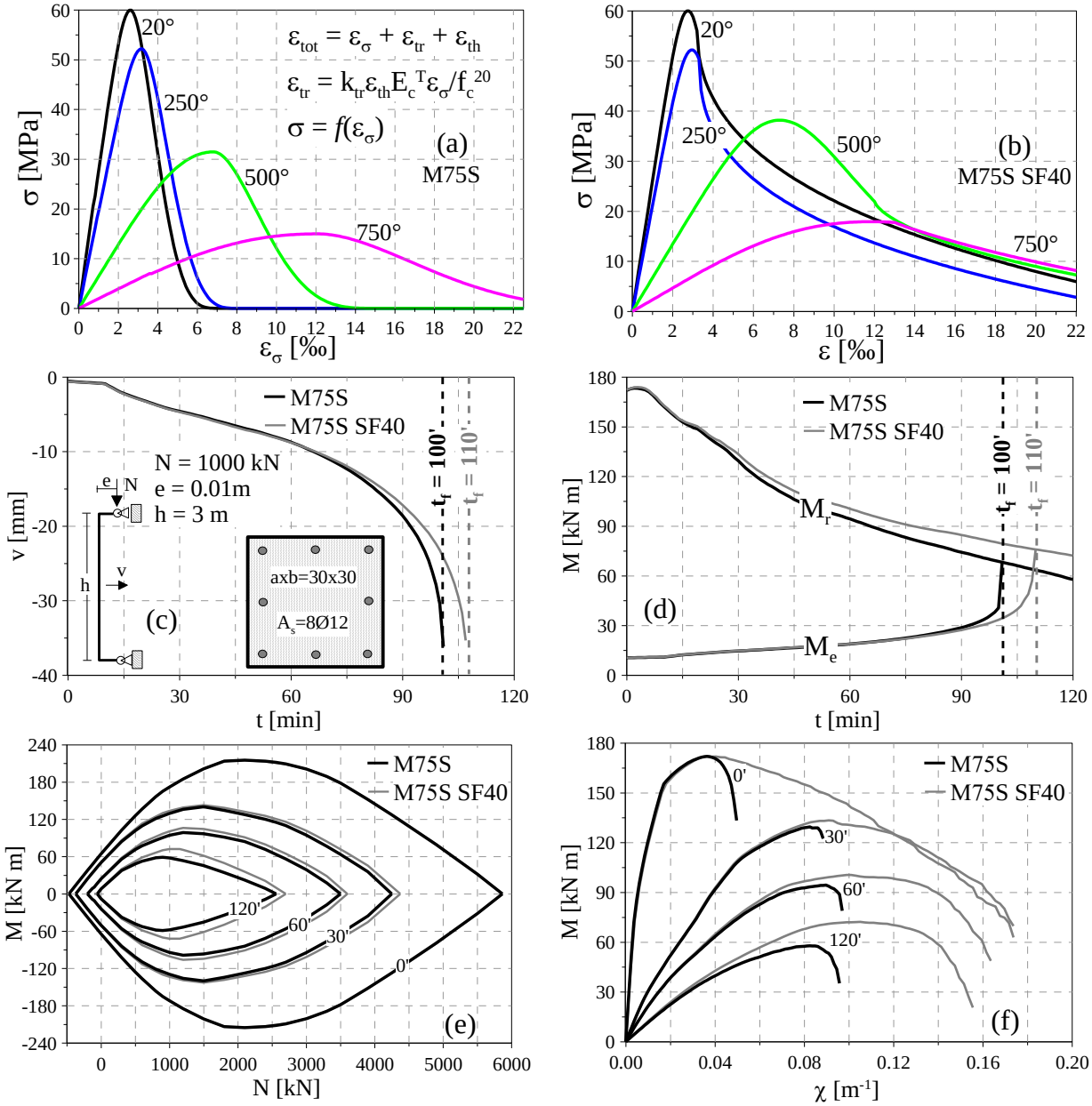

Figure 5: Plots of the analytical formulations of the stress-strain laws (a,b); geometry, restraints and curves of the displacement vs. fire duration (c); resisting and applied moments vs. fire duration (d); moment-axial force envelopes (e); and moment-curvature diagrams (f).

6. CONCLUDING REMARKS

The results of this research project – where the volumetric fraction of the cementitious matrix was strictly controlled and kept constant in all the seven mixes under investigation – confirm that polypropylene fibers do not significantly influence concrete stress-strain curves in compression, as well as its strength and elastic modulus in a high-temperature context. (Concrete spalling due to moisture, thermal gradients and applied loads is not treated in this paper). For the same fiber content, however, fibrillated fibers are slightly advantageous both in residual and hot conditions. As expected, hooked steel fibers are much more effective, as they markedly increase not only the compressive strength and the elastic modulus after cooling, but also – and more – the compressive strength at high temperature.

From the structural point of view, in the case of heavily-loaded R/C columns in fire the worked example shows that even small amounts of steel fibers can markedly increase column ductility, while the effect of the fibers on M-N envelopes and on fire resistance is rather limited. It is fair to say, however, that pp and steel fibers offer other advantages – not discussed in this paper – like greater concrete resistance to spalling at high temperature.

7. ACKNOWLEDGEMENTS

The authors are indebted to CTG-Italcementi Group (Bergamo, Italy) for the financial support given to this research project under the grant "Thermo-mechanical Sensitivity and Spalling in HPC Exposed to High Temperature" (2012-2015).

8. REFERENCES

[1] fib Bulletin No.46, "Fire Design of Concrete Structures – Structural Behaviour and Assessment", *Commission 4 "Modelling of Structural Behaviour and Design", Task Group 4.3 "Fire Design of Concrete Structures", Working Party 4.3-2 - Convener Luc Taerwe (May 2008)*, 214 pp.

[2] Bamonte P. and Gambarova P.G., "Properties of Concrete Subjected to Extreme Thermal Conditions", *Journal of Structural Fire Engineering*, 5 (1) (2014), 47-62.

[3] Felicetti R. and Gambarova P.G., "Effects of High Temperature on the Residual Compressive Strength of Siliceous HSCs", *ACI-Materials Journal*, 95 (4) (1998), 395-406.

[4] Jansson R. and Boström L., "Fire Spalling of Concrete – A Re-Assessment of Test Data", *8th Int. Conf. on Structures in Fire – SIF'14, Shanghai - China (June 2014)*, V.1, 297-304.

[5] Bamonte P. and Gambarova P.G. "Thermal and Mechanical Properties at High Temperature of a Very High-Strength Durable Concrete", *ASCE - Journal of Materials in Civil Engineering*, 22 (6) (2010), 545-555.

[6] Rossino C., Lo Monte F., Cangiano S., Felicetti R. and Gambarova P.G., "Concrete Spalling Sensitivity versus Microstructure: the Effects of Polypropylene Fibers and Aggregate Type", *3rd Int. Workshop on Concrete Spalling due to Fire Exposure, Paris – France (Sept. 2013)*, 1-9.

[7] Kodur V. and McGrath R., Fire Endurance of High-Strength Concrete Columns", *Fire Technology*, 39 (1), 73-87.

[8] Bamonte P. and Lo Monte F., "Reinforced-Concrete Columns Exposed to Standard Fire: Comparison among Different Constitutive Models for Concrete at High temperature", *Fire Safety Journal*, 71 (2015), 310-323.

[9] Nafarieh A.R., "Tunnels in Fire: Structural and Materials Behavior and Modeling", *Ph.D. dissertation defended in February 2011, Dept. of Structural Engrg., Politecnico di Milano*, Milan (Italy), 269 pp.